



ISTITUTO NAZIONALE DI RICERCA METROLOGICA Repository Istituzionale

Experimental quantum enhanced optical interferometry

Original

Experimental quantum enhanced optical interferometry / Genovese, M.. - In: AVS QUANTUM SCIENCE. - ISSN 2639-0213. - 3:4(2021), p. 044702. [10.1116/5.0062114]

Availability:

This version is available at: 11696/72930 since: 2025-02-17T15:22:29Z

Publisher:

AIP Publishing

Published

DOI:10.1116/5.0062114

Terms of use:

This article is made available under terms and conditions as specified in the corresponding bibliographic description in the repository

Publisher copyright


AIP

This article may be downloaded for personal use only. Any other use requires prior permission of the author and AIP Publishing. This article may be found at DOI indicated above.

(Article begins on next page)

REVIEW ARTICLE | NOVEMBER 24 2021

Experimental quantum enhanced optical interferometry

M. Genovese 



AVS Quantum Sci. 3, 044702 (2021)

<https://doi.org/10.1116/5.0062114>



Articles You May Be Interested In

Generation of two types of nonclassical optical states using an optical parametric oscillator with a PPKTP crystal

Appl. Phys. Lett. (November 2016)

Nonclassical light and metrological power: An introductory review

AVS Quantum Sci. (November 2019)

Programmable photon pair source

APL Photonics (January 2022)



Advance your science and career as a member of

AVS

LEARN MORE



Experimental quantum enhanced optical interferometry

Cite as: AVS Quantum Sci. **3**, 044702 (2021); doi: [10.1116/5.0062114](https://doi.org/10.1116/5.0062114)

Submitted: 2 July 2021 · Accepted: 13 September 2021 ·

Published Online: 24 November 2021



View Online



Export Citation



CrossMark

M. Genovese

AFFILIATIONS

Istituto Nazionale di Ricerca Metrologica, Strada delle Cacce 91, 10135, Torino, Italy and INFN, Sezione di Torino, via P. Giuria 1, 10125 Torino, Italy

ABSTRACT

Optical quantum interferometry represents the oldest example of quantum metrology, and it is at the source of quantum technologies. The original squeezed state scheme is now a significant element of the last version of gravitational wave detectors, and various additional uses have been proposed. Further quantum-enhanced schemes, from the SU(1,1) interferometer to twin beam correlation interferometry, have also reached the stage of proof of principle experiments, thus enlarging the field of experimental quantum interferometry and paving the way to several additional applications, from Planck scale signals search to small effect detection. In this review, I will describe these experimental achievements, and I will focus on their schemes, advantages, applications, and possible further developments.

Published under an exclusive license by AIP Publishing. <https://doi.org/10.1116/5.0062114>

TABLE OF CONTENTS

I. INTRODUCTION	1
II. GENERAL INTRODUCTION TO QUANTUM ENHANCED INTERFEROMETRY	2
III. SQUEEZED LIGHT ENHANCED INTERFEROMETERS	2
IV. SU(1,1) AND OTHER NONLINEAR INTERFEROMETERS	4
V. QUANTUM ENHANCED CORRELATION INTERFEROMETERS	6
VI. FURTHER IDEAS AND PERSPECTIVES	8
VII. CONCLUSIONS	10

I. INTRODUCTION

In the last two decades, a second quantum revolution, based on exploiting peculiar properties of single quantum states, prompted the emerging of quantum technologies, ranging from quantum information to quantum metrology.¹ Substantial progress has been made in the development of quantum-enhanced measurement in the last years. Quantum metrology is the new discipline addressed to overcome the limits of classical measurements, such as shot noise,^{2,3} by exploiting specific properties, and, in particular, peculiar correlations of quantum systems, as entanglement,⁴ discord,⁵ or squeezing.⁶ As other quantum technologies (e.g., quantum information, quantum computation, quantum communication, etc.) it had exponential growth in the last

20 years, due to the realization of several interesting proofs of principle experiments, mostly in quantum optics. Now this discipline is approaching practical applications ranging from biology to remote detection.^{7–12} As consolidated potentialities of this discipline one can mention, without any pretension to be exhaustive, the possibility of enhancing the performances of interferometers,^{13–21} of phase estimation,²² of object detection or testing,^{23–26} of super-resolution,^{27,28} of spectroscopy,²⁹ and of beating shot noise in imaging^{3,8,30,31} or absorption measurements.^{32,33}

In particular, the application of quantum-enhanced (or quantum-inspired) schemes to optical interferometry, a technique of huge widespread application ranging from basic science^{34,35} to computation,³⁶ represents the oldest example of quantum metrology, and it is at the very source of quantum technologies. Nowadays, the advantage of using squeezed light in interferometers has found application in enhancing the sensitivity of the upgraded version of gravitational wave experiments as GEO 600,^{37,38} LIGO,³⁴ and VIRGO,³⁵ while new ideas are reaching proof of the principle stage. In this review paper, the author will introduce the main elements of Experimental Quantum Enhanced Optical Interferometry, touching the following arguments:

- General introduction to quantum enhanced interferometry
- Squeezed light enhanced interferometers
- SU(1,1) interferometers
- Quantum-enhanced correlation interferometers
- New ideas and perspectives
- Conclusions

Further applications of quantum interferometry addressing quantum imaging, absorption measurement, etc. are beyond the purpose of this paper and can be found, for instance, in Refs. 8 and 39.

II. GENERAL INTRODUCTION TO QUANTUM ENHANCED INTERFEROMETRY

Nowadays, interferometers represent probably the most sensitive instruments we dispose of. Nevertheless, several kinds of noise must be coped for reaching the highest sensitivity.⁴⁰ Just for mentioning the ones considered by LIGO collaboration:⁴¹ thermal noise, seismic noise, Newtonian noise, laser frequency noise, laser intensity noise, auxiliary length control noise, actuator noise, alignment control noise, beam jitter noise, scattered light noise, residual gas noise, photodetector dark noise, etc.

Anyway, even when all these sources of noise are tamed, intrinsic limits remain. In particular, the classical interferometer sensitivity scales as $1/\sqrt{N}$ where N is the number of photons (i.e., scales with the square root of the inputted light intensity), the so-called shot noise.

Surprisingly enough, this limit can eventually be beaten by exploiting peculiar quantum properties of light,⁴² i.e., by inputting light states with specific properties of quantum systems (as squeezing or entanglement).^{43,44} In this last case, the phase sensitivity $\Delta\theta$ can eventually reach the so-called Heisenberg limit, i.e., a $1/N$ scaling. A limit generically imposed by the laws of quantum mechanics, namely, the generalized Heisenberg uncertainty $\Delta N\Delta\theta \geq 1$.⁴⁵⁻⁵⁷ It is worth noting that even this limit can eventually be beaten in the presence of prior information^{58,59} or should be refined in specific situations. Indeed, Hofmann⁶⁰ suggested considering the limit

$$\Delta\theta^2 \geq 1/\langle n^2 \rangle, \tag{1}$$

where the average of the squared photon number $\langle n^2 \rangle$ appears. This allows a better sensitivity in the case of large photon number fluctuations, $\Delta n^2 = \langle n^2 \rangle - \langle n \rangle^2 > 0$. However, the effective possibility of using this advantage is still under discussion.⁶¹

In general, the possibility of beating classical limits in interferometry represents one of the most intriguing chances offered by quantum metrology. These techniques are now overpassing the stage of theoretical proposals,^{62,63} reaching experimental applications (in some cases beyond proof of principle demonstrations). A few emblematic examples will be presented and discussed in the following.

III. SQUEEZED LIGHT ENHANCED INTERFEROMETERS

As mentioned, the first proposal of quantum-enhanced measurement was the idea of Caves¹³ concerning the use of squeezed states for improving the performances of interferometers under the shot noise. In real situations, eventually other technical noises can be more important than shot noise. Nonetheless, this proposal finally found an important application in gravitational wave detectors.

The idea is relatively simple. In a “traditional” interferometer, a laser beam (well approximated by a coherent state) enters a port of the system and propagates inside the interferometer splitting into two (or eventually more) components that at the end are recombined and interfere according to the relative acquired phase θ .

Let us consider for example a Mach-Zehnder interferometer (but the same considerations apply mutatis mutandis to any other interferometer), see Fig. 1. Let call 0 and 1 the two modes entering the initial beam splitter (BS). After propagation in the two arms, acquiring a

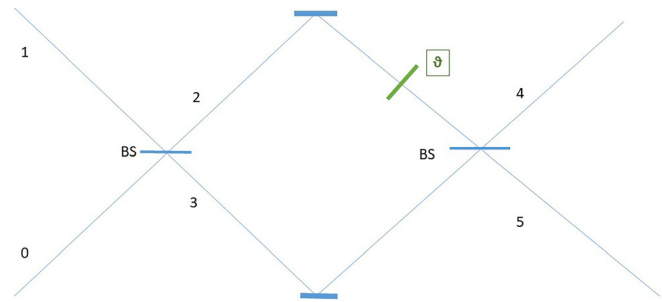


Fig. 1. Schematics of a Mach-Zehnder interferometer.

relative phase θ , they recombine on a second beam splitter, whose outputs we denote with modes 4 and 5. The photon destruction operator corresponding to mode 5 can thus be written in terms of the operators relative to the input modes 0, 1 as

$$a_5 = ie^{i\theta/2} \cdot (a_1 \sin(\theta/2) + a_0 \cos(\theta/2)). \tag{2}$$

Thus, if the mode 1 is a coherent state $|\alpha\rangle = D(\alpha)|vacuum\rangle$ (much more intense than the state inputting mode 0), where $D(\alpha) = \exp(\alpha a - \alpha^* a^\dagger)$, the output photon number in mode 5, $\langle n_5 \rangle = \langle a_5^\dagger a_5 \rangle$, is

$$\langle n_5 \rangle = \sin^2(\theta/2)|\alpha|^2 + \sin(\theta/2)\cos(\theta/2)|\alpha|(a_0 e^{-i\theta} + a_0^\dagger e^{i\theta}). \tag{3}$$

$X_\theta = 1/\sqrt{2}(a_0 e^{-i\theta} + a_0^\dagger e^{i\theta})$ being the quadrature variable (in the following $X_0 = X$).

If, on the same line, we evaluate the variance of n_5 we obtain

$$\langle \Delta n_5^2 \rangle = (\sin(\theta/2)\cos(\theta/2)|\alpha|)^2 \langle \Delta X^2 \rangle. \tag{4}$$

If the port 0 is unused, i.e., the input is the vacuum state, $|vacuum\rangle$, then $\langle \Delta X^2 \rangle = 1/4$. This represents the shot noise.

Caves demonstrated¹³ that inputting on the port 0 a squeezed state $D(\alpha)S(z)|vacuum\rangle$, where $S(z) = \exp[1/2(a^2 z^* - (a^\dagger)^2 z)]$, $z = re^{i\phi}$ (e.g., the squeezed vacuum $S(z)|vacuum\rangle$) then

$$\langle \Delta X^2 \rangle = e^{-(2r)}/4, \tag{5}$$

i.e., the noise is reduced with respect to the shot noise (a detailed mathematical analysis of shot noise, and in general of noise in interferometers, can be found in Ref. 40).

This result represented a fundamental advance, showing how the use of quantum resources, in the case the squeezing (see Ref. 64 for an introductory discussion of the use of squeezing in quantum sensing) can lead to an improvement with respect to classical limits, in this case the shot noise.

This upshot is related to the specific quantum properties of squeezed states. When considering quadrature variables, $X = 1/\sqrt{2}(a + a^\dagger)$ and $Y = 1/(\sqrt{2}i)(a - a^\dagger)$, the variances for the vacuum are $\Delta X = \Delta Y = 1/2$. The same variances characterize the coherent states that in the complex-amplitude plane are just translated vacuum (see Fig. 2). On the other hand, for squeezed states the variance in one quadrature is “squeezed,” e.g., $\Delta X = 1/2e^{-r}$, while for the other increases, $\Delta Y = 1/2e^r$, keeping their product fixed to 1/4. By combining a squeezed and a coherent state on a beam splitter antibunched

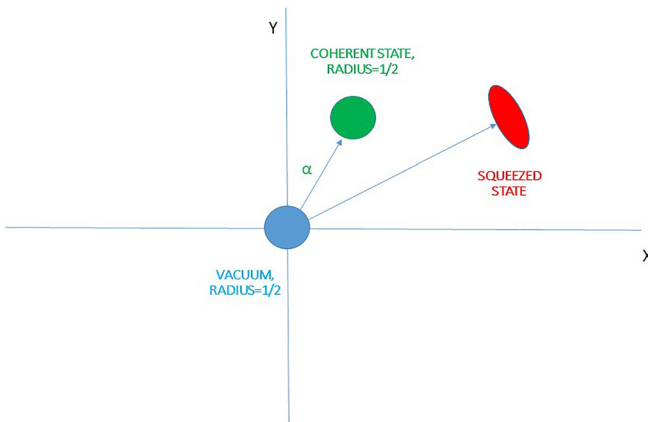


Fig. 2. Uncertainty circle in complex-amplitude state for vacuum, coherent state $|\alpha\rangle$, and squeezed state.

light can be produced, where eventually there are increased amplitude fluctuations and better defined phases.¹³ Incidentally, by combining two squeezed states on a beam splitter a photon number entangled state is obtained (a two-mode squeezed state).⁶⁵

A first experimental realization of Caves’ idea was achieved in Ref. 66, where an increase in the signal-to-noise ratio of 3.0 dB relative to the shot-noise limit was demonstrated. This result represented a milestone demonstrating, at least in a proof of principle experiment, the possible advantage of the use of quantum light in interferometry. In Ref. 67, a 2 dB increase in signal-to-noise ratio relative to the shot-noise was achieved in a polarization interferometer.

In the last years, the interest in these techniques has grown very rapidly thanks to their use for practical applications. After that, in Ref. 16, a 2.3 dB improvement was experimentally demonstrated in a power recycled Michelson with squeezed light injected into the dark port. This method found large interest in the development of extremely sensitive interferometers for gravitational wave search. Indeed, following the use in Geo 600,^{37,38} it found also application in LIGO,³⁴ where it now represents a significant component.⁴¹

With respect to previous versions, now in LIGO the squeezed vacuum source (an optical parametric oscillator, OPA) is placed inside the vacuum envelope on a separate suspended platform, reducing in this way the squeezing ellipse phase noise and backscattered light noise. Furthermore, the squeezer has been fully integrated into the automated lock acquisition sequence. Thanks to these improvements, above 50 Hz the interferometer sensitivity is increased by 2.0 and 2.7 dB at LIGO Hanford Observatory and LIGO Livingston Observatory, respectively.⁴¹ Thus, while improving interferometer sensitivity by increasing the input power to the interferometer is limited by radiation pressure (which induces instabilities and absorption of the test masses), injecting squeezed vacuum improves the signal-to-noise ratio by decreasing the interferometer noise. In this sense, 3 dB of squeezing is equivalent to doubling the intracavity power to 450 kW. For instance, this provides a 12% and 14% increase in binary neutron star in the spiral range at each respective site.⁴¹ Similar improvements have also been obtained into the other big gravitational wave detector, Virgo.³⁵

Nonetheless, below 50 Hz, injecting frequency-independent squeezed vacuum increases the quantum radiation pressure noise. This effect in LIGO limits at the moment a further increase of the current squeezing level. Frequency dependent squeezing could alleviate this problem.

Beyond these technical limits (e.g., contribution to radiation pressure noise), also losses are a significant problem,⁶⁸ since they reduce the squeezing.^{69,70} The conundrum of keeping a strong squeezing by coping losses without increasing the squeezing level can eventually be solved by amplifying the squeezing quadrature, where the information is encoded.⁷¹ A scheme overcoming external losses has been recently realized with a Mach-Zehnder like interferometer,⁷² demonstrating a 6 dB sub shot noise sensitivity even for 50% detection efficiency.

Coming back to the trade-off between radiation pressure noise and shot noise reduction, some idea for improving both, by realizing frequency dependent squeezing, has recently emerged. The point is that quantum fluctuations in the amplitude quadrature of the light generate a fluctuating radiation pressure on mirrors that in turn couples amplitude and phase quadratures⁷³

$$a_{out}^{phase} = a_{in}^{phase} - Ka_{in}^{amp} + signal, \tag{6}$$

where the Kimble factor K depends on the frequency (beyond the line width of the detector, the light power, and the mass of mirror).

The radiation pressure noise (dominating at low frequency) can be reduced by squeezing the amplitude quadrature and the shot noise (dominating the high-frequency sensitivity) demands for squeezing the phase quadrature. In Ref. 74, it was suggested a method for realizing this situation, based on generating EPR (Einstein-Podolsky-Rosen) entangled beams⁴³ through a detuned OPA. The method takes advantage of the entanglement between fields around the half of the pump frequency: measuring on the correlated modes allows reducing the uncertainty on the other (conditional squeezing), while being idler and signal fields separated by tens of MHz, it will not mix with the strong carrier to produce radiation pressure on mirrors. This scheme has been recently demonstrated in a proof of principle experiment.⁷³

Further semiclassical methods for improving gravitational wave detectors, in particular for getting rid of back-action fluctuations, can be found in Ref. 40, such as speed meter interferometers^{75–85} (performing quantum nondemolition measurements of mirror velocity), coupling to another (quantum-enhanced) interferometer^{86,87} or white-light cavity schemes (i.e., broadening the bandwidth).⁸⁸

Before concluding this section, it is worth mentioning that a further theoretical progress was the demonstration of Ref. 89 that the choice of the average relative number of photons as a phase estimator is not optimal (albeit the simplest one and “feasible” with current technology). Indeed, further information about the true value of the phase shift (PS) is contained in the quantum fluctuations of the number of particles measured at the output ports. In brief, the combination of coherent and squeezed light at the input beam splitter creates an entangled state that a suited measure could further exploit. Theoretical considerations, based on the Cramér-Rao bound, lead to the bound [p being the number of measurements and $F(\theta)$ the Fisher information]

$$\Delta\theta = \frac{1}{\sqrt{pF(\theta)}} = \frac{1}{\sqrt{p(|\alpha|^2 e^{2r} + \sinh^2(r))}}. \tag{7}$$

The Heisenberg scaling

$$\Delta\theta = \frac{1}{\sqrt{pN}}, \tag{8}$$

is reached when $|\alpha|^2 \simeq \sinh^2(r) \simeq N/2$ and $p, N \ll 1$.

Finally, the possibility of improving interferometry in the presence of losses by exploiting a phase-sensitive amplifier on the outputs was discussed and experimentally demonstrated for a coherent state input in Ref. 90, while further a few theoretical ideas, that could lead to improvements in a more far future, emerged, concerning the use of intelligent states,^{91–93} extended squeezed states,⁹⁴ or other methods.^{95–98}

IV. SU(1,1) AND OTHER NONLINEAR INTERFEROMETERS

Nonlinear interferometers, i.e., interferometers where nonlinear optical effects (eventually exploiting quantum resources) are considered (see Ref. 39 for an earlier review), are another very interesting case. In a general sense, one can exploit interference connected to nonlinear media for several purposes;³⁹ for instance, one could measure the optical dispersion of a material placed in between two nonlinear sources, tailoring specific quantum states, measuring the absorption in the nonlinear crystal, achieving spectroscopy, or realizing imaging protocols.

The most significant example of an interferometer based on the use of nonlinear optical media is the so-called SU(1,1) interferometer (see Ref. 99 for an earlier review, in particular on quantum noise performances), whose name derives from the different transformation performed with respect to the SU(2)-type interaction, realized by a beam splitter in a traditional interferometer. Here, the beam splitters are substituted by parametric amplifiers (PAs), where the two outputs (usually dubbed idler and signal) of the first PA are recombined in the second PA. This scheme has been demonstrated to be able to reach the Heisenberg scaling $1/N$ (in terms of photon number N) in Ref. 100.

Indeed, when defining the generators of SU(2) in terms of input mode annihilation operators

$$J_1 = (a_0^\dagger a_1 + a_1^\dagger a_0)/2, \tag{9}$$

$$J_2 = -i(a_0^\dagger a_1 - a_1^\dagger a_0)/2, \tag{10}$$

$$J_3 = (a_0^\dagger a_0 - a_1^\dagger a_1)/2, \tag{11}$$

the beam splitter with transmissivity $\cos(\alpha/2)$ corresponds to the related group transformation $U = e^{-i\alpha J_1}$.

On the other hand, by defining the SU(1,1) algebra generators

$$K_1 = (a_0^\dagger a_1^\dagger + a_1 a_0)/2, \tag{12}$$

$$K_2 = -i(a_0^\dagger a_1^\dagger - a_1 a_0)/2, \tag{13}$$

$$K_3 = (a_0^\dagger a_0 + a_1 a_1^\dagger)/2, \tag{14}$$

the PA is described by the relative group element $U = e^{-2irK_2}$.

By considering the sequence of transformations describing a traditional interferometer (Mach–Zehnder, Fabry–Pérot, or what else), one obtains the usual $\sim 1/\sqrt{N}$ sensitivity;^{46,100} while, similarly to the squeezed state interferometers, also SU(1,1) interferometers can achieve a phase sensitivity of $1/N$, but in this case with only vacuum fluctuations entering the input ports and coherent states pumping the active devices.

The original proposal¹⁰⁰ was based on spontaneous emission (i.e., the parametric amplifier had the input modes as vacuum states): this is not very effective due to the limitation in the intensity (i.e., in N) of the output modes. Thus, experimental realizations follow a scheme where coherent states are injected.^{101,102}

The details of the experimental setup, and the possible eventual applications, depend on the medium chosen as the parametric amplifier. At the moment, three different configurations have been realized: exploiting four-wave mixing in atom vapors cells,^{103–107} bulk crystals,¹⁰⁸ or nonlinear optical fibers.^{109–111}

The general idea of a SU(1,1) interferometer is, as mentioned, to substitute the beam splitters with parametric amplifiers, see Fig. 3, whose Hamiltonian is (in parametric approximation where the pump field is approximated to a classical field)

$$H_{PA} = i(ga_1^\dagger a_2^\dagger - g^* a_1 a_2). \tag{15}$$

Introducing the gain $G_j = \cosh(kg)$, k being a constant, with $j = 1, 2$ denoting the first or second PA, when a coherent state $|\alpha\rangle$ is inputted in mode 1 (while the other input mode is in the vacuum) the output intensities are

$$I_4 = |\alpha|^2 (G_1^2 G_2^2 + (G_1^2 - 1)(G_2^2 - 1) + 2G_1 G_2 \sqrt{G_1^2 - 1} \sqrt{G_2^2 - 1} \cos(\theta_1 + \theta_2)), \tag{16}$$

$$I_5 = |\alpha|^2 (G_1^2 \cdot (G_2^2 - 1) + G_2^2 \cdot (G_1^2 - 1) + 2G_1 G_2 \sqrt{G_1^2 - 1} \sqrt{G_2^2 - 1} \cos(\theta_1 + \theta_2)), \tag{17}$$

where θ_1 and θ_2 are the phases acquired on the arms 1 and 2 of the interferometer, respectively.

One interesting property that differentiates a SU(1,1) interferometer from a usual Mach–Zehnder is, as can be immediately evinced from Eq. (3), that the interference fringes depend on the sum of θ_1 and θ_2 (instead of depending on the difference). More interestingly, the fringe size depends quadratically (thanks to amplification) on the phase sensing field strength, to be compared to a linear dependence of the linear interferometer. Finally, another significant difference is that for the SU(1,1) interferometer making the difference between the two outputs the phase dependence is canceled.

However, the most interesting property of a SU(1,1) interferometer is that the noise is not amplified as much as the signal, increasing the signal-to-noise ratio (an amplifier at the output of a usual interferometer would amplify in the same way signal and noise).

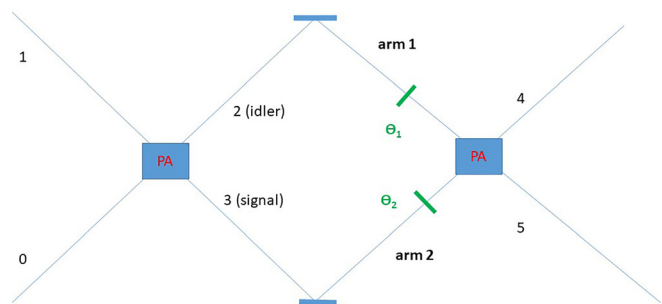


FIG. 3. Schematics of a SU(1,1) interferometer.

Indeed, if one measures the quadrature variable,¹⁰¹ the result is

$$\langle \Delta^2 X \rangle = |G_1 G_2 + (G_1^2 - 1)(G_2^2 - 1)e^{i(\theta_1 + \theta_2)}|^2, \quad (18)$$

reaching a minimum at the dark fringe $(\theta_1 + \theta_2) = \pi$ for all quadrature variables (at variance with squeezed state interferometry, where only one quadrature experiences noise reduction).

One can then evaluate the relative signal to noise ratio (SNR) for a quadrature measurement for a small change δ in the phase in one arm is [in the case $(G_2^2 - 1) \gg (G_1^2 - 1)$]¹¹²

$$\text{SNR} = \frac{\langle Y \rangle^2}{\langle \Delta^2 Y \rangle} = 2 \left[G_1 + \sqrt{G_1^2 - 1} \right] \cdot |\alpha|^2 \delta^2, \quad (19)$$

which provides a $[G_1 + \sqrt{G_1^2 - 1}]/2$ enhancement respect to a traditional interferometer. A result that is substantially unaffected by detection inefficiencies (or other losses outside the interferometer).^{104,108,113} On the other hand, it is not insensitive to losses inside the interferometer.¹⁰²

The first experimental realization of a SU(1,1) interferometer was achieved in Ref. 103, where the two parametric amplifiers were based on a four-wave mixing process in ⁸⁵Rb vapor cells 12 mm long. They were, respectively, illuminated by an intense vertically polarized pump beam (400 mW) from a frequency-stabilized Ti:sapphire laser locked to a Fabry–Perot reference cavity. Furthermore, a horizontally polarized seed beam was combined with the pump beam at an angle of 0.7 in the center of the first vapor cell. The pump laser frequency was about 0.8 GHz blue detuned from the ⁸⁵Rb $F = 2 \rightarrow F'$ transition at 795 nm, and the seed signal beam was about 3.04 GHz red-shifted from the pump with an acoustic optic modulator. The amplified signal and the conjugate idler beams of the first cell were addressed into the second vapor cell where they were symmetrically crossed with the pump, similar to the first vapor cell. The two output beams, from the second vapor cell, were then measured demonstrating a quadratic fringe intensity dependence on the intensity of the phase sensing field at high gain.

A second example, where the quantum effects were considered in detail with respect to the classical analysis of Ref. 103, is Ref. 104. Here again, the two PAs were realized with four-wave-mixing in ⁸⁵Rb atoms pumped with beams deriving from a titanium-sapphire laser. Thanks to the amplification at the second PA, the fringe size of the nonclassical interferometer was enhanced by 7.4 dB with respect to a classical Mach–Zehnder interferometer at the same illumination level, leading to a 4 dB advantage in signal-to-noise ratio in phase measurement (mostly limited by losses inside the interferometer).

As a third example, based on parametric down-converted (PDC), one can consider the experimental implementation of Ref. 17 (see also Ref. 108). Here, the interferometer consisted of two cascaded 3 mm long β -barium borate (BBO) crystals (the first placed on a translational stage for controlling the interferometer phase) cut for collinear frequency degenerate type-I phase matching. The pump was the second harmonic of a 400 nm laser with a 5 kHz repetition rate, 1.5 ps pulses. The multimode PDC light generated by the SU(1,1) interferometer was then spatially and spectrally filtered before being detected. In this realization of the SU(1,1) interferometer both the outputs of the first PA cross the same medium producing the same phase change. An advantage of this configuration is that random phase fluctuations (e.g., caused by air flow, temperature fluctuations, etc.) wipeout, since the

three fields (idler, signal and pump) copropagate. One of the main results of this work is the demonstration of the insensitivity to losses: for specific gain choices the phase estimation was under shot noise up to 80% losses, see Fig. 4. This kind of interferometer was then further investigated^{114,115} and, in particular, extended to a wide field SU(1,1) interferometer.¹¹⁶

The idea of a dual-beam interferometer (collinear, but nondegenerate PDC with two independent measurements) was then considered theoretically in Ref. 112 (see also Ref. 117) and experimentally in Ref. 118. Since the SU(1,1) interferometer fringes depend on the sum of the phases acquired by the two beams, this configuration allows optimizing the measurement, achieving the same SNR of squeezed state interferometry.

To point toward real applications of SU(1,1) interferometers is mandatory to increase the intensity. In Ref. 119, a pumped-up version of SU(1,1) interferometer using all particles (particularly suited for atomic interferometers) was proposed, while in Ref. 120 a bright seeded SU(1,1) interferometer was realized, where the pump beams generated by a titanium-sapphire laser were injected in ⁸⁵Ru vapor cells. This last experiment led to a 1.15 dB advantage with respect to the standard noise limit, where losses lowered the expected advantage,

$$\sqrt{G^2(1-G)^2/(G^2 + (1-G)^2)} \quad (\text{with } 1/\sqrt{N} \text{ scaling}), \text{ of 2.6 dB.}$$

An alternative for overcoming the limited intensity power, which remains the most severe drawback of this kind of interferometers, was recently suggested and realized considering a configuration where a SU(2) interferometer is nested in a SU(1,1) one.¹²¹ In more detail, the signal beam of the first PA is fed into the dark port of a SU(2) (a Mach–Zehnder) interferometer, while an intense coherent state is fed on the other port. The light emerging from the dark port of this SU(2) interferometer is then recombined with the idler beam in the second PA. The experiment, with two ⁸⁵Rb cells generating four-wave mixing, led to a 2.2(5) dB advantage that was substantially maintained even with a 1 mW power.

Concluding this section it is worth mentioning a few further proposals suggesting “variations” on the theme of the SU(1,1) interferometer.^{122–127}

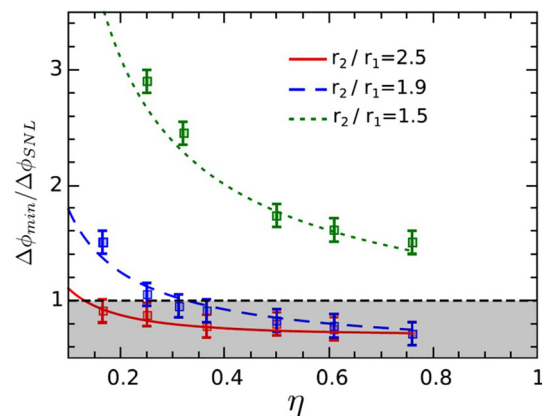


Fig. 4. Reprinted figure with permission from Manceau *et al.*, Phys. Rev. Lett. 119, 223604 (2017). Copyright 2017, American Physical Society. Best phase sensitivity normalized to shot noise against the detection transmission η . The curves correspond to different parametric gains.

In Ref. 122, the second PA is substituted by a beam splitter (in this case of course idler and signal beam must have the same wave length) followed by a homodyne detection leading substantially to the same SNR of Eq. (19).

In Ref. 123, it was theoretically studied the phase sensitivity of a SU(1,1) interferometer with a coherent state in one input port and a squeezed-vacuum state in the other input port using the method of homodyne detection, showing the potentiality of achieving the Heisenberg limit.

Finally, we mention that, on the one hand, in Ref. 124 it was demonstrated, theoretically and experimentally, that the second PA can eventually be substituted by two homodyne detections (with the same local oscillator) combining the relative photocurrents. On the other hand, in Ref. 125 the application to stochastic phase estimation was studied, and in Ref. 126, a theoretical analysis of a multimode integrated SU(1,1) interferometer was performed. In Ref. 128, the effect of additional external resources was investigated, and in the very recent Ref. 129, it was shown the possibility of combining the two photodetector outputs with an optimal weight factor for beating the shot noise by the same amount, regardless of the phase shift in the interferometer. Further recent theoretical ideas (exploiting quantum resources as Fock states or parity measurements) can be found in Refs. 130–132.

V. QUANTUM ENHANCED CORRELATION INTERFEROMETERS

One more significant application of quantum light concerns the possibility of enhancing the performances of correlation interferometry.

In particular, in the last years, the interest for correlation interferometry grew in connection to the possible application to the search of quantum gravity effects. Indeed, the dream of building a theory unifying general relativity and quantum mechanics, the so-called quantum gravity, has been a key element in theoretical physics research for the last 60 years: several attempts in this sense have been considered. However, for many years, no testable prediction emerged from these studies, leading to the common wisdom that this kind of research was more properly a part of mathematics than of physics, being by construction unable to produce experimentally testable predictions as required by the Galilean scientific method. In the last few years this common wisdom was challenged.^{133–138} In particular, it has been proposed that Planck scale effects, connected to noncommutativity of position variables in different directions,^{139,140} could be measured, for instance in cavities with microresonators¹³⁷ or in two coupled interferometers,¹³⁶ the so-called “holometer.”

This possibility led to the building of the 40 m Fermilab holometer^{141–143} that recently started to pose limits (2.1×10^{-20} m/ $\sqrt{\text{Hz}}$) on the possible noise stemming from these effects^{141,143} in the 1–6 MHz region.

In synthesis, a holometer is a device consisting of two Michelson interferometers (MIs), that are spatially close. The purpose of the holometer is to search for a particular type of correlated noise, which is conjectured to arise from gravitational effects at the Planck scale, affecting the two spatially close interferometers as relative phase noise. A little more in detail, the idea at the basis of these studies is that non-commutativity at the Planck scale ($l_p = 1.616 \times 10^{-35}$ m) of position variables in different directions, predicted by several Planck scale physics models,^{144,145} generates an additional very weak phase noise, referred to as holographic noise (HN). In a single interferometer, this

noise substantially confounds with other sources of noise, even when the most sensible gravitational wave interferometers are considered,¹³⁶ since by construction their HN resolution is worse than their resolution to gravitational-wave at low frequencies. Nevertheless, when the two equal interferometers of the holometer have overlapping space-time volumes, then the HN between them is correlated and can be identified easier.¹³⁶ Since the ultimate limit for holometer sensibility, as for any classical-light based apparatus, is dictated by the shot noise, the possibility of going beyond this limit by exploiting quantum optical states is of the utmost interest.^{3,9,146–148}

Beyond this application, measuring relative phase noise could find use in the detection of the gravitational wave background^{149–152} or in finding traces of primordial black holes.^{153,154}

The use of quantum light in correlation interferometry was firstly investigated in Refs. 155 and 156.

For this purpose, it was considered that the observable measured at the output of the holometer is described by an appropriate operator $\hat{C}(\phi_1, \phi_2)$, ϕ_k being the phase shift (PS) detected by the interferometer I_k , $k = 1, 2$, with expectation value $\langle \hat{C}(\phi_1, \phi_2) \rangle = \text{Tr}[\rho_{12} \hat{C}(\phi_1, \phi_2)]$, where ρ_{12} is the overall density matrix associated with the state of the two light beams injected in I_1 and I_2 .

In the Fermilab scheme, the idea for observing the eventual existence of the HN is comparing $\langle \hat{C}(\phi_1, \phi_2) \rangle$ in two different experimental configurations of I_1 and I_2 , namely, when the arms are parallel, “||”, or perpendicular, “⊥”.¹³⁶ Indeed, according to Ref. 136, one expects that HN is correlated in the first case (being the arms in the same light cone), while it is not in the second case.

Thus, on the one hand, in the configuration || the correlation of the interference fringes would highlight the presence of the HN.

On the other hand, the configuration ⊥ serves as a reference measurement, namely, it corresponds to the situation where the correlation due to HN is absent. In other words, it is equivalent to estimating the “background.”

In general, being the statistical properties of the PS fluctuations due to HN described by a suitable probability density function, $f_x(\phi_1, \phi_2)$, $x = ||, \perp$, the expectation of any operator $\hat{O}(\phi_1, \phi_2)$ is obtained by averaging over f_x , namely, $\langle \hat{O}(\phi_1, \phi_2) \rangle \rightarrow \mathcal{E}_x[\hat{O}(\phi_1, \phi_2)] \equiv \int \langle \hat{O}(\phi_1, \phi_2) \rangle f_x(\phi_1, \phi_2) d\phi_1 d\phi_2$.

Since in the holometer the HN can be observed through a correlation between two phases, the appropriate function to be estimated is their covariance

$$\mathcal{E}_{||}[\delta\phi_1 \delta\phi_2] \approx \frac{\mathcal{E}_{||}[\hat{C}(\phi_1, \phi_2)] - \mathcal{E}_{\perp}[\hat{C}(\phi_1, \phi_2)]}{\langle \partial_{\phi_1, \phi_2}^2 \hat{C}(\phi_{1,0}, \phi_{2,0}) \rangle}, \quad (20)$$

$$(\delta\phi_1, \delta\phi_2 \ll 1).$$

$\delta\phi_k = \phi_k - \phi_{k,0}$, $\phi_{k,0}$ being the mean PS value measured by I_k , $k = 1, 2$ reducing as much as possible the associated uncertainty

$$\mathcal{U}^{(0)} = \frac{\sqrt{2 \text{Var}[\hat{C}(\phi_{1,0}, \phi_{2,0})]}}{|\langle \partial_{\phi_1, \phi_2}^2 \hat{C}(\phi_{1,0}, \phi_{2,0}) \rangle|}, \quad (21)$$

where $\text{Var}[\hat{C}(\phi_{1,0}, \phi_{2,0})] = \langle \hat{C}(\phi_{1,0}, \phi_{2,0})^2 \rangle - \langle \hat{C}(\phi_{1,0}, \phi_{2,0}) \rangle^2$ does not depend on the PS fluctuations due to the HN, but it represents the intrinsic quantum fluctuations of the measurement described by the

operator $\hat{C}(\phi_1, \phi_2)$ and depends on the optical (quantum) states entering the holometer.

In Refs. 155 and 156 it was demonstrated that, when the two input modes of each interferometer I_k , $k = 1, 2$, are excited in a coherent state and a squeezed vacuum state with the mean number of photons μ and λ , respectively

$$\mathcal{U}_{\text{SQ}}^{(0)}(\mu, \lambda) \approx \sqrt{2} \frac{\lambda + \mu(1 + 2\lambda - 2\sqrt{\lambda + \lambda^2})}{(\lambda - \mu)^2}. \quad (22)$$

As expected, in analogy with the PS measurement for a single interferometer,¹³ if $\mu \gg \lambda \gg 1$, then we have the optimal accuracy $\mathcal{U}_{\text{SQ}}^{(0)} \approx (2\sqrt{2}\lambda\mu)^{-1}$. This represents an evident advantage in terms of uncertainty reduction [of the order $(4\lambda)^{-1}$] with respect to the classical case $\mathcal{U}_{\text{CL}}^{(0)} \approx \sqrt{2}/\mu$ when only coherent states are employed. An important difference arises between the single interferometer PS measurement, involving a first order moment of the photon number distribution, and the covariance estimation, involving the second order moments: while in the first case the uncertainty scales as the usual standard quantum limit one, $\propto \mu^{-1/2}$, in the second case it scales $\propto \mu^{-1}$ (neglecting the little relative contribution of the squeezed state to the intensity).

Nonetheless, even a larger advantage was demonstrated when considering a configuration where second port input modes of I_1 and I_2 , a_1 and a_2 , are the component of a photon-number entangled beam, in particular a twin beam (or a two-mode squeezed vacuum state)^{157,158}

$$| \text{TWB} \rangle \rangle = (1 + \lambda)^{-1/2} \sum_n (1 + \lambda^{-1})^{-n/2} |n\rangle_{a_1} |n\rangle_{a_2}, \quad (23)$$

while two coherent states still enter into the other two ports. This correlation property leads to the amazing result that the contribution to the uncertainty coming from the photon number fluctuation noise is $\mathcal{U}_{\text{TWB}}^{(0)} = 0$ (when $\lambda, \mu \neq 0$) in the ideal situation of no losses, representing an ideal accuracy of the interferometric scheme to the PS covariance due to HN.

This advantage is conserved even in the presence of losses in the case of high quantum resources exploited, i.e., $\mu \gg \lambda \gg 1$, where one finds $\mathcal{U}_{\text{SQ}}^{(0)}/\mathcal{U}_{\text{CL}}^{(0)} \approx (1 - \eta) + \eta/(4\lambda)$ and $\mathcal{U}_{\text{TWB}}^{(0)}/\mathcal{U}_{\text{CL}}^{(0)} \approx 2\sqrt{5}(1 - \eta)$ when the total detection efficiency η is sufficiently large.

These theoretical ideas were then experimentally demonstrated in Ref. 159.

Both the two independent squeezed states and a twin-beam (TWB) like injection were considered. Each Michelson interferometer, with an arm length of 0.92 m, was fed with 1.5 mW of 1064 nm light from a low noise Nd:YAG laser source. This laser source was also used to seed the optical parametric oscillators generating the squeezing. The light for the MIs was spatially cleaned with an optical fiber. Then, each interferometer had two piezo-actuated high-reflectivity end mirrors ($R_M = 99.9\%$), while the partially reflecting mirrors for the two power recycling cavities had a reflectivity of $R_{\text{PRM}} = 90\%$.

The squeezed-light (6.5 dB relative to the shot noise), produced by a parametric down-conversion in a potassium titanyl phosphate

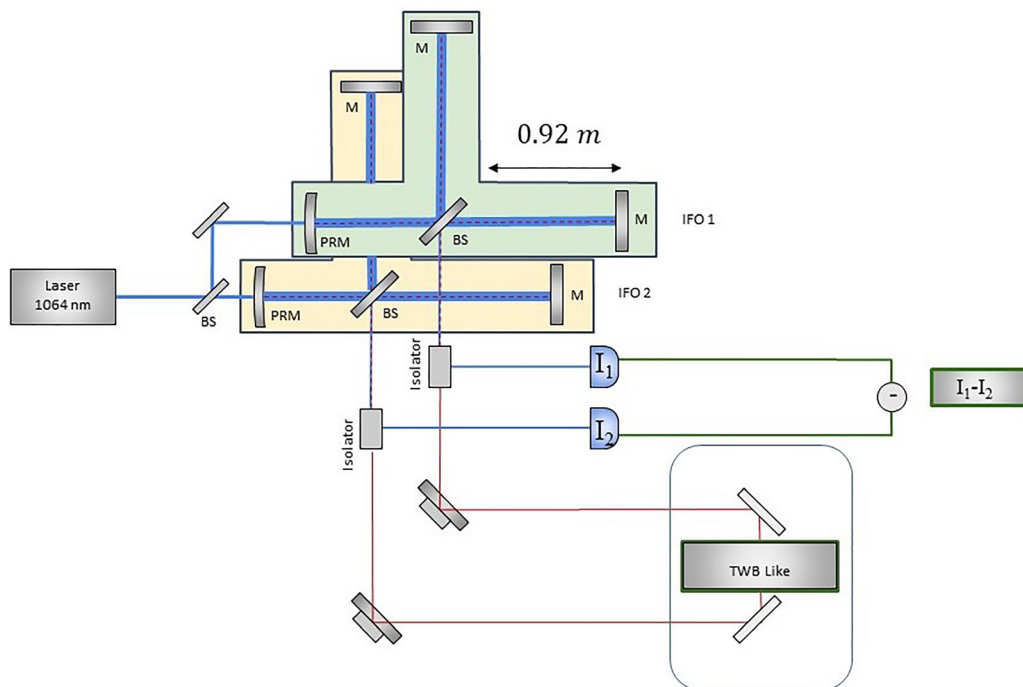


Fig. 5. Simplified schematic of the double-interferometer setup as described in Ref. 159 in the twin beams configuration. The two spatially close (~ 10 cm) interferometer input ports were fed 1064 nm laser light from a low noise Nd:YAG laser source. Each interferometer had a power recycling mirror (PRM) in the input port, to form a cavity around the interferometer. The input beams were split at a beam splitter (BS) in each interferometer and subsequently impinged on piezo-controlled end mirrors (M). A Faraday isolator in each output port allowed for measuring the output while twin-beam (TWB) modes were injected into the output ports.

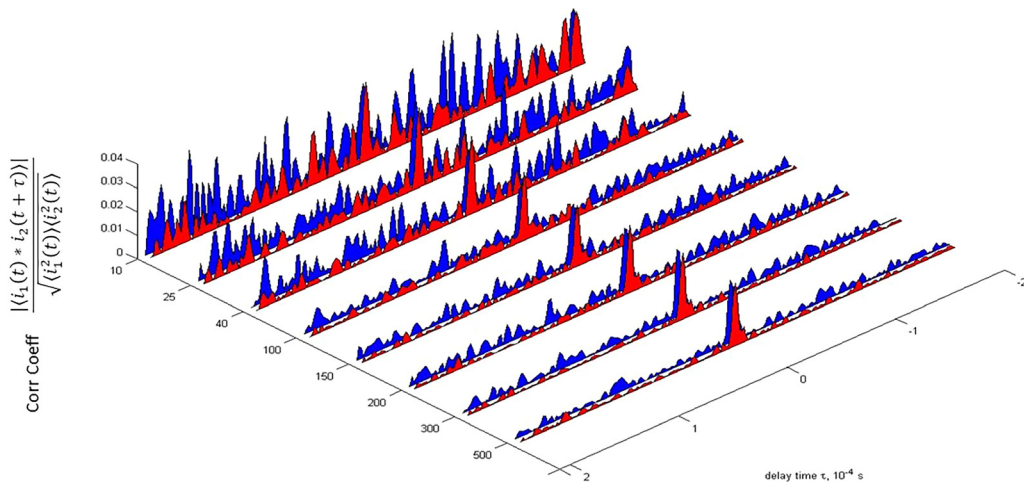


Fig. 6. Analysis of the time series obtained from the independent squeezer configuration from the experiment of Ref. 159, with added white noise (as described in Ref. 159). The red curves correspond to the squeezing injection configuration and the blue curves to the coherent case. The plot shows the cross-correlation of the data in the time domain versus the number of samples. The correlation peak is hidden in the noise for small sample numbers, equivalent to short acquisition time, and it emerges when the number of samples is increased. The use of squeezing allows clearly for earlier detection of the peak.

(PPKTP) crystal placed in a semi-monolithic linear cavity, was injected into the two MIs via their output ports.

The signal-to-noise ratio with squeezing injected was consistently higher, by a factor of 2, of the classical interferometer. In the spectral domain, correlated signals were extracted by the cross-linear spectral density of the two interferometers, demonstrating an improvement of a factor 1.35 from the injection of squeezed states. A result that also poses an upper limit on HN in the 13 MHz region ($3 \times 10^{-17} \text{ m}/\sqrt{\text{Hz}}$).

When a twin-beam-like signal was injected (see Fig. 5), the correlation between the two modes led to a noise reduction of 2.5 dB with respect to the SNL (Standard Noise Limit).

This enhancement was also observed in the power spectral density of the subtracted interferometer outputs Fig. 6, demonstrating that the presence of faint uncorrelated noise can be more easily detected by twin beam-like correlations and, therefore, the possible advantage offered by this technique in experiments of correlation interferometry.

Following this proof of principle experiment, very recently in Ref. 160 a detailed description of a tabletop quantum-enhanced holometer was presented (in the version based on the injection of two independent squeezed beams), with the purpose of realizing a new experiment on Planck scale effect search (Fig. 7).

Furthermore, interest emerged in investigating possible advantages of using non-Gaussian (as photon subtracted) states,¹⁶¹ while in Ref. 162 decoherence effects in this kind of experiment were analyzed.

VI. FURTHER IDEAS AND PERSPECTIVES

In conclusion, in this section we consider new schemes and ideas that, even if still far from practical applications, could eventually lead to interesting developments in a more or less next future.

A first line of research, somehow connected to SU(1,1) interferometers, is inserting nonlinear media in the arms of an interferometer for enhancing its performances.^{163–165} A first example was

experimentally realized in Ref. 163, where the performances of a Mach-Zehnder interferometer operating with single photons probes were enhanced by inserting a parametric amplifier in one arm, still scaling as $1/\sqrt{N}$. Very recently, a new experiment with two PAs, one per arm, was realized.¹⁶⁴ This setup allowed achieving a 5.6 dB squeezed noise floor under shot noise limit and a 4.9 dB enhancement of signal to noise ratio, reaching the Heisenberg limit.

Another very interesting seminal proposal,^{14,166,167} much discussed in the theoretical literature, is the use of photon number entangled states of the form

$$\frac{|N\rangle|0\rangle + |0\rangle|N\rangle}{\sqrt{2}}, \tag{24}$$

dubbed NOON states.

In synthesis, while using N independent photons in a two arms (a,b) interferometer one has

$$\left[\frac{|a\rangle + e^{i\theta}|b\rangle}{\sqrt{2}} \right]^{\otimes N}, \tag{25}$$

leading to a $1/\sqrt{N}$ phase uncertainty scaling, with a NOON state the phase cumulates as

$$\frac{|N\rangle_a|0\rangle_b + e^{iN\theta}|0\rangle_a|N\rangle_b}{\sqrt{2}}, \tag{26}$$

leading to a $1 + \cos(N\theta)$ interference dependence, which implies a $1/N$ scaling.¹⁶⁸ Albeit of large theoretical interest, unluckily no effective idea exists for creating high N photon NOON states with present technology, and only a few proof of principle experiments were realized with $N = 2$,^{169–174} (easily created by Hong–Ou–Mandel interference) or $N = 4$,^{175–177} (with postselection that, due to low probability success, limits an eventual practical use). Furthermore, the advantage offered by these states is very sensitive to losses.¹⁷⁸

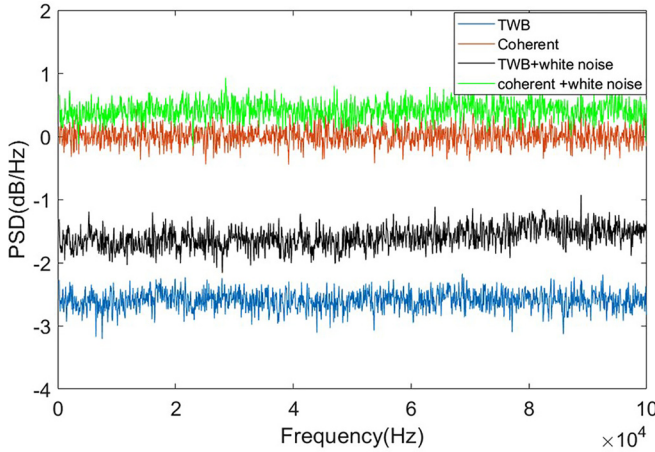


Fig. 7. Comparison of the power spectral densities of the photocurrent difference between the MI outputs of the experiment as described in Ref. 159, with and without TWB. Green and black traces have uncorrelated white noise introduced in the MIs, with and without TWB, respectively. The white noise clearly emerges in the TWB case demonstrating the efficiency of this method.

Also, the use of twin photon Fock states $|N, N\rangle$ would lead to asymptotically approaching Heisenberg limit.^{179–181} Nonetheless, also high N photon Fock states are far from being produced.¹⁸² Postselected heralded $N = 8$ Fock states are the present limit, Ref. 183. Moreover, in Ref. 183 they interfered the Fock states on a beam splitter to create generalized Holland–Burnett states, showing they perform almost as well as optimal states in a lossy scenario (i.e., much better than NOON states in this case).

Similar problems for the production concern maximally correlated states defined in Ref. 184, which would allow exactly reaching Heisenberg limit.

To overpass these difficulties, on the one hand, the use of twin beams coupled to photo-count measurements was suggested¹⁸⁵ and, in a simplified version, implemented.¹⁸⁶ In this proof of principle experimental realization, the photon-counting detection was realized through a multiplexed scheme; the measured data were then compared with what expected by a different phase shift impressed on the two components of the twin beam and a final detection described by a specific POVM (positive operator-valued measure) keeping into account the multiplexed measurement. The shot noise limit was surpassed despite a realistic level of losses. Very recently,¹⁸⁷ a new experiment further enhanced the advantage by using NIST (National Institute of Standards and Technology) transition-edge sensors.

On the other hand, new detection methods, suited for reaching Heisenberg limit with resources experimentally realizable (or even to beat $1/N$ scaling^{188–190}) including or not entangled states and/or nonlinear interactions,¹⁹¹ were considered. For instance, the Heisenberg scaling in phase estimation (where the unknown phase was implemented a birefringent element) was also reached in common spatial mode polarization interferometer (theoretically equivalent to a Mach–Zehnder one) by exploiting a generalized Kitaev’s algorithm, reaching a 10 dB advantage with respect to the standard quantum limit with highest number of resources (378 photons).¹⁹² Nevertheless, the extension to practical uses (i.e., a much larger number of photons) still remains far from reach.

A further class of proposals is based on using parity measurements,¹⁹³ i.e., on measuring the parity operator $\Pi = e^{i\pi a^\dagger a}$, which substantially requires photocounting detection. A first proposal in this sense appeared in Ref. 194: here it was suggested using collinear degenerate twin beams, Eq. (23), i.e., two mode squeezed vacuum (TMSV), entering one port of the interferometer, e.g., 1 in Fig. 1, and performing a parity measurement to one output port, e.g., 4 in Fig. 1. This leads to

$$\langle \Pi \rangle_{\theta+\pi/2} = \frac{1}{\sqrt{1 + \bar{n}(\bar{n} + 2) \sin^2 \theta}}, \quad (27)$$

where \bar{n} is the average photon number of the TMSV, which, through Cramér–Rao bound, leads to a $1/\sqrt{\bar{n}(\bar{n} + 2)}$ dependence for the phase uncertainty in the proximity of $\theta = 0$. This result even beats the Heisenberg limit: here is an example of application of the Hofmann limit,⁶⁰ Eq. (1), since $\Delta n^2 = \langle n^2 \rangle - \langle n \rangle^2 = \bar{n}^2 + 2\bar{n}$ for TMSV.

The Heisenberg limit can eventually be beaten also through nonlinear transformations.¹⁹⁵ For example, this limit can be overcome when the generator of the transformation is proportional to the photon number. In Ref. 196, a Kerr type $e^{i\theta(a^\dagger a)^2}$ transformation was considered leading to a $\Delta\theta \sim 1/N^{3/2}$ scaling, besides a finite detection efficiency only represents a multiplicative factor to this scaling. More in general a Hamiltonian including all possible k -body couplings allows a $1/N^k$ scaling for entangled probe states and a $1/N^{k-1/2}$ scaling for a probe initially in a product state,^{188,195–197} representing in this last case also an interesting example of quantum-enhanced measurement without entanglement.^{198,199} Further theoretical optical schemes with nonlinear phase shifts can be found in Refs. 200 and 201.

Finally, different ideas emerged on using weak values or weak value-inspired methods^{202,203} in interferometry. Weak value measurements were introduced²⁰² in 1988 by Aharonov, Albert, and Vaidman, and they represent a new paradigm of quantum measurement. In summary, the weak value of an observable \hat{A} is defined as $\langle \hat{A} \rangle_w = \langle \psi_f | \hat{A} | \psi_i \rangle / \langle \psi_f | \psi_i \rangle$, where the key role is symmetrically played by the pre-selected ($|\psi_i\rangle$) and post-selected ($|\psi_f\rangle$) quantum states. For evaluating weak values, one considers the von Neumann coupling between the observable \hat{A} and the pointer observable \hat{P} , corresponding to the measuring classical apparatus, in the weak coupling regime. Due to this weak coupling, so little information is extracted from a single measurement that the state does not collapse. According to the unitary transformation $\hat{U} = \exp(-ig\hat{A} \otimes \hat{P})$, in this weak interaction regime the evolution of the system is

$$\langle \psi_f | e^{-ig\hat{A} \otimes \hat{P}} | \psi_i \rangle \simeq \langle \psi_f | \psi_i \rangle (1 - ig\langle \hat{A} \rangle_w \hat{P}). \quad (28)$$

Thus, weak values are measurable quantities and can provide an “amplification” in measuring a small parameter g (e.g., a phase),^{6,202,204–212} which can be significantly useful in the presence of technical noise.²¹³

For example, in Ref. 214 it was demonstrated (both theoretically and experimentally in a Sagnac configuration) that it is possible reaching the same sensitivity of balanced homodyne detection measuring the dark port only. This could allow a general improvement of sensitivity by allowing a large reduction of the intensity at the detector. This method was recently extended in Ref. 215.

As mentioned, weak value amplification finds significant use in the presence of technical noise. On this line, in Ref. 216 it was demonstrated that weak values can be applied to reduce systematic uncertainties in phase estimation. Specifically, it was considered the case of a Sagnac interferometer where the beam splitter is substituted by a polarizing beam splitter and the phase is encoded in one of the polarizations. The experiment demonstrated a 30 times phase resolution improvement. A further approach exploiting weak values appeared in Ref. 217. Here, it was considered a Michelson (or Mach-Zehnder) interferometer with a “stable” polarization-dependent phase shift in one arm. In this case, the preselected state is (in terms of Horizontal, H, and vertical, V, polarization states) of the form $(|H\rangle + |V\rangle)/\sqrt{2}$ and the postselection is $(\cos\alpha|H\rangle + \sin\alpha|V\rangle)$, while the polarization measurement operator is, for instance, $\hat{A} = |H\rangle\langle H|$. The uncertainty is amplified as the signal by the weak value $\langle \hat{A} \rangle_w$, but a small weak value attenuates phase and uncertainty at the same time. Thus, the reduction of the uncertainty is achieved by exploiting a feedback control: a $\sim 10^{-3}$ reduction factor was experimentally demonstrated.

Thus, in summary, several new ideas are emerging for further improving optical (and not only) interferometry. Many of them already were demonstrated in proof of principle experiments. However, if and which of them will really find practical applications, overcoming present limitations, remains to be clarified.

VII. CONCLUSIONS

In the panorama of quantum technologies, quantum metrology represents one of the most significant candidates for practical applications in an advanced stage. In particular, quantum-enhanced optical interferometry has already found significant use in gravitational wave detectors. Furthermore, several other methods have already overpassed the stage of theoretical proposals, as they have been realized at least in proof of principle experiments, that are prompting new applications of these methods, for example in correlation interferometry.

The theoretical and experimental studies in this area are further promoted by new proposals of applications that range from technological needs, in sensing or computation or else, to fundamental physics. Some of them already reached significant practical applications nowadays, as gravitational wave detection, others are addressing more visionary ideas that could be of interest in the next or farther future, ranging from the Planck scale effects^{142,218–220} up to wormhole search.²²¹

ACKNOWLEDGMENTS

This work has received funding from the European Commission's PATHOS EU H2020 FET-OPEN Grant No. 828946 and Horizon 2020, from the EMPIR Participating States in the context of the Project No. 17FUN01 “BeCOMe.”

AUTHOR DECLARATIONS

Conflict of Interest

The authors have no conflicts to disclose.

DATA AVAILABILITY

Data sharing is not applicable to this article as no new data were created or analyzed in this study.

REFERENCES

- ¹Quantum Information, Computation and Cryptography, edited by F. Benatti (Springer, New York, 2010).
- ²P. Moreau *et al.*, *Nat. Rev. Phys.* **1**, 367 (2019).
- ³G. Brida, M. Genovese, and I. R. Berchera, *Nat. Photonics* **4**, 227 (2010).
- ⁴J. P. Dowling, *Contemp. Phys.* **49**, 125 (2008).
- ⁵K. Modi *et al.*, *Phys. Rev. X* **1**, 021022 (2011).
- ⁶R. Schnabel, *Phys. Rep.* **684**, 1 (2017).
- ⁷S. Pirandola *et al.*, *Nat. Photonics* **12**, 724 (2018).
- ⁸M. Genovese, *J. Opt.* **18**, 073002 (2016).
- ⁹V. Giovannetti, S. Lloyd, and L. Maccone, *Science* **306**, 1330 (2004); *Nat. Photonics* **5**, 222 (2011).
- ¹⁰S. Olivares, *Riv. Nuovo Cimento* **6**, 341 (2018).
- ¹¹C. L. Degen *et al.*, *Rev. Mod. Phys.* **89**, 035002 (2017).
- ¹²G. Petrini *et al.*, *Adv. Quantum Technol.* **3**, 2000066 (2020).
- ¹³C. M. Caves, *Phys. Rev. D* **23**, 1693 (1981).
- ¹⁴A. Boto *et al.*, *Phys. Rev. Lett.* **85**, 2733 (2000).
- ¹⁵S. F. Huelga *et al.*, *Phys. Rev. Lett.* **79**, 3865 (1997).
- ¹⁶K. McKenzie *et al.*, *Phys. Rev. Lett.* **88**, 231102 (2002).
- ¹⁷M. Manceau *et al.*, *Phys. Rev. Lett.* **119**, 223604 (2017).
- ¹⁸G. Toth and I. Apellaniz, *J. Phys. A* **47**, 424006 (2014).
- ¹⁹M. Paris, *Int. J. Quantum. Inf.* **07**, 125 (2009).
- ²⁰M. Malitesta *et al.*, [arXiv:2109.09178](https://arxiv.org/abs/2109.09178).
- ²¹L. Pezze and A. Smerzi, e-print [arXiv:1411.5164](https://arxiv.org/abs/1411.5164); “Atom interferometry,” in *Proceedings of the International School of Physics “Enrico Fermi,” Course 188, Varenna*, edited by G. M. Tino and M. A. Kasevich (IOS, Amsterdam, 2014), p. 691.
- ²²A. Berni *et al.*, *Nat. Photonics* **9**, 577 (2015).
- ²³S. Lloyd, *Science* **321**, 1463 (2008).
- ²⁴S. Tan, B. Erkmen, V. Giovannetti, S. Guha, S. Lloyd, L. Maccone, S. Pirandola, and J. Shapiro, *Phys. Rev. Lett.* **101**, 253601 (2008).
- ²⁵E. Lopaeva *et al.*, *Phys. Rev. Lett.* **110**, 153603 (2013).
- ²⁶G. Ortolano *et al.*, *Sci. Adv.* **7**, eabc7796 (2021); E. Losero *et al.*, [arXiv:2102.09428](https://arxiv.org/abs/2102.09428).
- ²⁷M. D’Angelo *et al.*, *Phys. Rev. Lett.* **87**, 13602 (2001).
- ²⁸G. Bjork *et al.*, *Phys. Rev. Lett.* **86**, 4516 (2001).
- ²⁹D. A. Kalashnikov *et al.*, *Nat. Photonics* **10**, 98 (2016).
- ³⁰G. Brida, M. Genovese, A. Meda, and I. R. Berchera, *Phys. Rev. A* **83**, 033811 (2011).
- ³¹N. Samantaray *et al.*, *Light Sci. Appl.* **6**, e17005 (2017).
- ³²J. Sabines-Chesterking *et al.*, *Phys. Rev. Appl.* **8**, 014016 (2017).
- ³³E. Losero *et al.*, *Sci. Rep.* **8**, 7431 (2018).
- ³⁴J. Aasi *et al.*, *Nat. Photonics* **7**, 613 (2013).
- ³⁵F. Acernese *et al.*, *Phys. Rev. Lett.* **123**, 231108 (2019).
- ³⁶G. Wetzstein *et al.*, *Nature* **588**, 39 (2020).
- ³⁷J. Abadie *et al.*, *Nat. Phys.* **7**, 962 (2011).
- ³⁸H. Grote, K. Danzmann, K. L. Dooley, R. Schnabel, J. Slutsky, and H. Vahlbruch, *Phys. Rev. Lett.* **110**, 181101 (2013).
- ³⁹M. V. Chekhova and Z. Y. Ou, *Adv. Opt. Photonics* **8**, 104 (2016).
- ⁴⁰S. L. Danilishin *et al.*, *Living Rev. Relativ.* **22**, 4835 (2019).
- ⁴¹A. Buikema *et al.*, *Phys. Rev. D* **102**, 062003 (2020).
- ⁴²F. Dell’Anno *et al.*, *Phys. Rep.* **428**, 53 (2006).
- ⁴³M. Genovese, *Phys. Rep.* **413**, 319 (2005).
- ⁴⁴C. Fabre and N. Treps, *Rev. Mod. Phys.* **92**, 35005 (2020).
- ⁴⁵Z. Y. Ou, *Phys. Rev. A* **55**, 2598 (1997); *Phys. Rev. Lett.* **77**, 2352 (1996).
- ⁴⁶B. Yurke, S. L. McCall, and J. R. Klauder, *Phys. Rev. A* **33**, 4033 (1986).
- ⁴⁷B. C. Sanders and G. J. Milburn, *Phys. Rev. Lett.* **75**, 2944 (1995).
- ⁴⁸A. Luis and J. Perina, *Phys. Rev. A* **54**, 4564 (1996).
- ⁴⁹L.-Z. Liu *et al.*, *Nat. Photon.* **15**, 137 (2021).
- ⁵⁰G. S. Summy and D. T. Pegg, *Opt. Commun.* **77**, 75 (1990).
- ⁵¹D. W. Berry, H. M. Wiseman, and J. K. Breslin, *Phys. Rev. A* **63**, 053804 (2001); D. W. Berry, B. L. Higgins, S. D. Bartlett, M. W. Mitchell, G. J. Pryde, and H. M. Wiseman, *ibid.* **80**, 052114 (2009).
- ⁵²M. J. W. Hall, *J. Mod. Opt.* **40**, 809 (1993).
- ⁵³M. Hayashi, *Prog. Inf.* **8**, 81 (2011).
- ⁵⁴L. Maccone and A. Ricciardi, *Quantum* **4**, 292 (2020).
- ⁵⁵R. Demkowicz-Dobrzanski, K. Banaszek, and R. Schnabel, *Phys. Rev. A* **88**, 041802(R) (2013).

- ⁵⁶J. Söderholm *et al.*, *Phys. Rev. A* **67**, 053803 (2003).
- ⁵⁷B. G. Englert *et al.*, *Int. J. Quantum Inf.* **6**, 129 (2008).
- ⁵⁸P. M. Anisimov, G. M. Raterman, A. Chiruvelli, W. N. Plick, S. D. Huver, H. Lee, and J. P. Dowling, *Phys. Rev. Lett.* **104**, 103602 (2010).
- ⁵⁹V. Giovannetti, S. Lloyd, and L. Maccone, *Phys. Rev. Lett.* **108**, 260405 (2012).
- ⁶⁰H. F. Hofmann, *Phys. Rev. A* **79**, 033822 (2009).
- ⁶¹V. Giovannetti and L. Maccone, *Phys. Rev. Lett.* **108**, 210404 (2012).
- ⁶²R. Demkowicz-Dobrzanski, M. Jarzyna, and J. Kolodynski, *Prog. Opt.* **60**, 345 (2015).
- ⁶³T. Kaple *et al.*, *Proc. SPIE* **6603**, 660316 (2005).
- ⁶⁴B. J. Lawrie *et al.*, *ACS Photonics* **6**, 1307 (2019).
- ⁶⁵M. S. Kim *et al.*, *Phys. Rev. A* **65**, 032323 (2002).
- ⁶⁶M. Xiao, L.-A. Wu, and H. J. Kimble, *Phys. Rev. Lett.* **59**, 278 (1987).
- ⁶⁷P. Grangier, R. E. Slusher, B. Yurke, and A. LaPorta, *Phys. Rev. Lett.* **59**, 2153 (1987).
- ⁶⁸Incidentally losses are usually significantly affecting all quantum technologies protocols (with the significant exception of quantum illumination Refs. 23–25).
- ⁶⁹J. Gea-Banacloche and G. Leuchs, *J. Opt. Soc. Am. B* **4**, 1667 (1987).
- ⁷⁰X. Zhang *et al.*, *Phys. Rev. A* **88**, 013838 (2013).
- ⁷¹M. Manceau, F. Khalili, and M. Chekhova, *New J. Phys.* **19**, 013014 (2017).
- ⁷²G. Frascella *et al.*, *npj Quantum Inf.* **7**, 72 (2021).
- ⁷³J. Südbek *et al.*, *Nat. Photonics* **14**, 240 (2020).
- ⁷⁴Y. Ma *et al.*, *Nat. Phys.* **13**, 776 (2017).
- ⁷⁵V. B. Braginsky and F. Y. Khalili, *Phys. Lett. A* **147**, 251 (1990).
- ⁷⁶Y. Chen, *Phys. Rev. D* **67**, 122004 (2003).
- ⁷⁷S. L. Danilishin, *Phys. Rev. D* **69**, 102003 (2004).
- ⁷⁸M. Wang *et al.*, *Phys. Rev. D* **87**, 096008 (2013).
- ⁷⁹T. Zhang, *et al.*, *New J. Phys.* **20**, 103040 (2018).
- ⁸⁰V. B. Braginsky *et al.*, *Phys. Rev. D* **61**, 044002 (2000).
- ⁸¹P. Purdue, *Phys. Rev. D* **66**, 022001 (2002).
- ⁸²P. Purdue and Y. Chen, *Phys. Rev. D* **66**, 122004 (2002).
- ⁸³A. R. Wade *et al.*, *Phys. Rev. D* **86**, 062001 (2012).
- ⁸⁴S. H. Huttner *et al.*, *Classical Quantum Gravity* **34**, 024001 (2017).
- ⁸⁵E. Knyazev *et al.*, *Phys. Lett. A* **382**, 2219 (2018).
- ⁸⁶B. Julsgaard, A. Kozhokin, and E. S. Polzik, *Nature* **413**, 400 (2001).
- ⁸⁷C. B. Moller *et al.*, *Nature* **547**, 191 (2017).
- ⁸⁸A. Wicht *et al.*, *Opt. Commun.* **134**, 431 (1997).
- ⁸⁹L. Pezzè and A. Smerzi, *Phys. Rev. Lett.* **100**, 073601 (2008).
- ⁹⁰N. Spagnolo *et al.*, *Phys. Rev. Lett.* **108**, 233602 (2012).
- ⁹¹M. Hillery and L. Mlodinow, *Phys. Rev. A* **48**, 1548 (1993).
- ⁹²C. Brif and A. Mann, *Phys. Rev. A* **54**, 4505 (1996).
- ⁹³V. Perinova, A. Luks, and J. Krepelka, *J. Opt. B* **2**, 81 (2000).
- ⁹⁴F. A. Raffa, M. Rasetti, and M. Genovese, *J. Phys. A* **52**, 475301 (2019).
- ⁹⁵D. Gatto, P. Facchi, and V. Tamma, *Int. J. Quantum Inf.* **18**, 1941019 (2020).
- ⁹⁶E. Zeuthen *et al.*, *Phys. Rev. D* **100**, 062004 (2019).
- ⁹⁷J.-Y. Wu *et al.*, *Phys. Rev. A* **100**, 013814 (2019).
- ⁹⁸S. Olivares *et al.*, *Quantum Meas. Quantum Metrol.* **3**, 38 (2016).
- ⁹⁹Z. Y. Ou and X. Li, *APL Photonics* **5**, 080902 (2020).
- ¹⁰⁰J. Liu *et al.*, *New J. Phys.* **22**, 013031 (2020).
- ¹⁰¹W. N. Plick *et al.*, *New J. Phys.* **12**, 083014 (2010).
- ¹⁰²Z. Y. Ou *et al.*, *Phys. Rev. A* **85**, 023815 (2012).
- ¹⁰³J. Jing, C. Liu, Z. Zhou, Z. Y. Ou, and W. Zhang, *Appl. Phys. Lett.* **99**, 011110 (2011).
- ¹⁰⁴F. Hudelist, J. Kong, C. Liu, J. Jing, Z. Y. Ou, and W. Zhang, *Nat. Commun.* **5**, 3049 (2014).
- ¹⁰⁵J. M. Lukens, N. A. Peters, and R. C. Pooser, *Opt. Lett.* **41**, 5438 (2016).
- ¹⁰⁶B. E. Anderson, P. Gupta, B. L. Schmittberger, T. Horrom, C. Hermann-Avigliano, K. M. Jones, and P. D. Lett, *Optica* **4**, 752 (2017).
- ¹⁰⁷W. Du *et al.*, *Opt. Lett.* **43**, 1051 (2018).
- ¹⁰⁸P. R. Sharapova, O. V. Tikhonova, S. Lemieux, R. W. Boyd, and M. V. Chekhova, *Phys. Rev. A* **97**, 053827 (2018).
- ¹⁰⁹X. Guo, N. Liu, X. Li, Y. Liu, and Z. Y. Ou, *Sci. Rep.* **6**, 30214 (2016).
- ¹¹⁰J. M. Lukens, R. C. Pooser, and N. A. Peters, *Appl. Phys. Lett.* **113**, 091103 (2018).
- ¹¹¹Y. Liu, J. Li, L. Cui, N. Huo, S. M. Assad, X. Li, and Z. Y. Ou, *Opt. Express* **26**, 27705 (2018).
- ¹¹²J. Li, Y. Liu, L. Cui, N. Huo, S. M. Assad, X. Li, and Z. Y. Ou, *Phys. Rev. A* **97**, 052127 (2018).
- ¹¹³J. Li, Y. Liu, N. Huo, L. Cui, C. Feng, Z. Y. Ou, and X. Li, *Opt. Express* **27**, 30552 (2019).
- ¹¹⁴S. Lemieux, M. Manceau, P. R. Sharapova, O. V. Tikhonova, R. W. Boyd, G. Leuchs, and M. V. Chekhova, *Phys. Rev. Lett.* **117**, 183601 (2016).
- ¹¹⁵G. Frascella, R. V. Zakharov, O. V. Tikhonova, and M. V. Chekhova, *Laser Phys.* **29**, 124013 (2019).
- ¹¹⁶G. Frascella, E. E. Mikhailov, N. Takanashi, R. V. Zakharov, O. V. Tikhonova, and M. V. Chekhova, *Optica* **6**, 1233 (2019).
- ¹¹⁷A. Ferreri *et al.*, *Quantum* **5**, 461 (2021).
- ¹¹⁸Y. Liu, N. Huo, J. Li, L. Cui, X. Li, and Z. Y. Ou, *Opt. Express* **27**, 11292 (2019).
- ¹¹⁹S. S. Szigeti *et al.*, *Phys. Rev. Lett.* **118**, 150401 (2017).
- ¹²⁰S. Liu *et al.*, *Phys. Rev. Appl.* **10**, 064046 (2018).
- ¹²¹W. Du *et al.*, e-print arXiv:2004.14266 (2020).
- ¹²²Z. Y. Ou, S. F. Pereira, and H. J. Kimble, *Appl. Phys. B* **55**, 265 (1992).
- ¹²³D. Li *et al.*, *New J. Phys.* **16**, 073020 (2014).
- ¹²⁴P. Gupta, B. L. Schmittberger, B. E. Anderson, K. M. Jones, and P. D. Lett, *Opt. Express* **26**, 391 (2018).
- ¹²⁵K. Zheng *et al.*, *Photonics Res.* **8**, 1653 (2020).
- ¹²⁶A. Ferreri *et al.*, e-print arXiv:2012.03751 (2021).
- ¹²⁷C. M. Caves, *Adv. Quantum Technol.* **3**, 1900138 (2020).
- ¹²⁸J. Liu *et al.*, *Opt. Express* **28**, 39443 (2020).
- ¹²⁹G. Shukla *et al.*, *Opt. Express* **29**, 95 (2021).
- ¹³⁰S. Chang *et al.*, e-print arXiv:2103.07844 (2021).
- ¹³¹S. Wang and J. Zhang, e-print arXiv:2104.09718 (2021).
- ¹³²S. Wang, J. Zhang, and X. Xu, e-print arXiv:2105.03820 (2021).
- ¹³³G. Amelino-Camelia *et al.*, *Nature* **393**, 763 (1998).
- ¹³⁴G. Amelino-Camelia, *Nature* **398**, 216 (1999).
- ¹³⁵G. Amelino-Camelia, *Nature* **478**, 466 (2011).
- ¹³⁶G. Hogan, *Phys. Rev. D* **85**, 064007 (2012).
- ¹³⁷I. Pikovski *et al.*, *Nat. Photonics* **8**, 393 (2012).
- ¹³⁸J. D. Bekenstein, e-print arXiv:1211.3816 (2012).
- ¹³⁹P. Aschieri and L. Castellani, *J. Geom. Phys.* **60**, 375 (2010).
- ¹⁴⁰P. Aschieri and L. Castellani, *J. High Energy Phys.* **2009**, 086.
- ¹⁴¹A. S. Chou *et al.*, *Phys. Rev. D* **95**, 063002 (2017).
- ¹⁴²L. Aiello *et al.*, arXiv:2108.04746.
- ¹⁴³A. Bisio *et al.*, *Ann. Phys.* **368**, 177 (2016).
- ¹⁴⁴C. Hogan and O. Kwon, e-print arXiv:1506.06808 (2017).
- ¹⁴⁵A. Bisio *et al.*, *Phys. Rev. Lett.* **113**, 200401 (2014).
- ¹⁴⁶A. Laucht *et al.*, *Nanotechnology* **32**, 162003 (2021).
- ¹⁴⁷G. Brida, M. Genovese, E. Monticone, C. Portesi, M. Rajteri, and I. R. Berchera, “Experimental sub-shot noise quantum imaging versus differential classical imaging,” in *Fourth International Conference on Quantum, Nano and Micro Technologies* (2010), pp. 71–76.
- ¹⁴⁸R. Schnabel, N. Mavalvala, D. E. McClelland, and P. K. Lam, *Nat. Commun.* **1**, 121 (2010).
- ¹⁴⁹J. D. Romano and N. J. Cornish, *Living Rev. Relativ.* **20**, 2 (2017).
- ¹⁵⁰T. Akutsu *et al.*, *Phys. Rev. Lett.* **101**, 101101 (2008).
- ¹⁵¹A. Nishizawa *et al.*, *Classical Quantum Gravity* **25**, 225011 (2008).
- ¹⁵²A. Shoda *et al.*, *Phys. Rev. D* **89**, 027101 (2014).
- ¹⁵³B. J. Carr and S. W. Hawking, *Mon. Not. R. Astron. Soc.* **168**, 399 (1974).
- ¹⁵⁴A. S. Chou *et al.*, *Classical Quantum Gravity* **34**, 165005 (2017).
- ¹⁵⁵I. Ruo Berchera, I. P. Degiovanni, S. Olivares, and M. Genovese, *Phys. Rev. Lett.* **110**, 213601 (2013).
- ¹⁵⁶I. Ruo-Berchera, I. P. Degiovanni, S. Olivares, N. Samantaray, P. Traina, and M. Genovese, *Phys. Rev. A* **92**, 053821 (2015).
- ¹⁵⁷A. Meda, E. Losero, N. Samantaray, F. Scafrimuto, S. Pradyumna, A. Avella, I. Ruo-Berchera, and M. Genovese, *J. Opt.* **19**, 094002 (2017).
- ¹⁵⁸I. P. Degiovanni and I. R. Berchera, *Metrologia* **56**, 024001 (2019).
- ¹⁵⁹S. T. Pradyumna *et al.*, *Commun. Phys.* **3**, 104 (2020).
- ¹⁶⁰S. M. Vermeulen *et al.*, e-print arXiv:2008.04957 (2021).
- ¹⁶¹N. Samantaray *et al.*, *Phys. Rev. A* **101**, 063810 (2020).
- ¹⁶²F. Benatti *et al.*, *Int. J. Quantum Inf.* **15**, 1740014 (2017).
- ¹⁶³C. Vitelli *et al.*, *Phys. Rev. Lett.* **105**, 113602 (2010).
- ¹⁶⁴X. Zuo *et al.*, *Phys. Rev. Lett.* **124**, 173602 (2020).

- ¹⁶⁵G.-F. Jiao *et al.*, *Phys. Rev. A* **102**, 033520 (2020).
- ¹⁶⁶B. Sanders, *Phys. Rev. A* **40**, 2417 (1989).
- ¹⁶⁷H. Uys and P. Meystre, *Phys. Rev. A* **76**, 013804 (2007).
- ¹⁶⁸S. F. Huelga *et al.*, *Appl. Phys. B* **67**, 723 (1998).
- ¹⁶⁹Y. Shih, *Free-Space Laser Communication and Laser Imaging II* (SPIE, 2002), Vol. 4821.
- ¹⁷⁰M. W. Mitchell, J. S. Lundeen, and A. M. Steinberg, *Nature* **429**, 161 (2004).
- ¹⁷¹X. Gao, [arXiv:2107.02740](https://arxiv.org/abs/2107.02740).
- ¹⁷²H. S. Eisenberg *et al.*, *Phys. Rev. Lett.* **94**, 090502 (2005).
- ¹⁷³E. Su *et al.*, *Phys. Rev. Lett.* **119**, 080502 (2017).
- ¹⁷⁴N. Thomas-Peter *et al.*, *Phys. Rev. Lett.* **107**, 113603 (2011).
- ¹⁷⁵T. Nagata *et al.*, *Science* **316**, 726 (2007).
- ¹⁷⁶P. Walther *et al.*, *Nature* **429**, 158 (2004).
- ¹⁷⁷I. Afek *et al.*, *Science* **328**, 879 (2010).
- ¹⁷⁸P. A. Knott *et al.*, *Phys. Rev. A* **90**, 033846 (2014).
- ¹⁷⁹C. F. Wildfeuer *et al.*, *Phys. Rev. A* **80**, 043822 (2009).
- ¹⁸⁰R. Okamoto *et al.*, *New J. Phys.* **10**, 073033 (2008).
- ¹⁸¹M. J. Holland and K. Burnett, *Phys. Rev. Lett.* **71**, 1355 (1993).
- ¹⁸²P. Zapletal *et al.*, e-print [arXiv:2012.08544](https://arxiv.org/abs/2012.08544) (2020).
- ¹⁸³G. S. Thekkadath *et al.*, *npj Quantum Inf.* **6**, 89 (2020).
- ¹⁸⁴J. J. Bollinger *et al.*, *Phys. Lett. A* **54**, R4649 (1996).
- ¹⁸⁵H. Cable and G. Durkin, *Phys. Rev. Lett.* **105**, 039901 (2010).
- ¹⁸⁶J. Matthews *et al.*, *npj Quantum Inf.* **2**, 16023 (2016).
- ¹⁸⁷C. You *et al.*, [arXiv:2011.02454](https://arxiv.org/abs/2011.02454) (2020).
- ¹⁸⁸S. Boixo *et al.*, *Phys. Rev. Lett.* **98**, 090401 (2007).
- ¹⁸⁹S. Choi and B. Sundaram, *Phys. Rev. A* **77**, 053613 (2008).
- ¹⁹⁰S. Roy and S. Braunstein, *Phys. Rev. Lett.* **100**, 220501 (2008).
- ¹⁹¹M. Napolitano *et al.*, *Nature* **447**, 486 (2011).
- ¹⁹²B. L. Higgins *et al.*, *Nature* **450**, 393 (2007).
- ¹⁹³R. J. Birrittella *et al.*, [arXiv:2008.08658](https://arxiv.org/abs/2008.08658) (2020).
- ¹⁹⁴A. Anisimov *et al.*, *Phys. Rev. Lett.* **104**, 121102 (2010).
- ¹⁹⁵A. Luis, *Phys. Lett. A* **329**, 8 (2004).
- ¹⁹⁶J. Beltran and A. Luis, *Phys. Rev. A* **72**, 045801 (2005).
- ¹⁹⁷S. Boixo *et al.*, *Phys. Rev. Lett.* **101**, 040403 (2008).
- ¹⁹⁸D. Braun *et al.*, *Rev. Mod. Phys.* **90**, 035006 (2018).
- ¹⁹⁹F. Benatti and D. Braun, *Phys. Rev. A* **87**, 012340 (2013).
- ²⁰⁰J. Joo *et al.*, *Phys. Rev. A* **86**, 043828 (2012).
- ²⁰¹C. Wei and Z. Zhang, *J. Mod. Opt.* **64**, 743 (2017).
- ²⁰²Y. Aharonov *et al.*, *Phys. Rev. Lett.* **60**, 1351 (1988).
- ²⁰³F. Piacentini *et al.*, *Nat. Phys.* **13**, 1191 (2017).
- ²⁰⁴O. Hosten and P. Kwiat, *Science* **319**, 787 (2008).
- ²⁰⁵K. J. Resch, *Science* **319**, 733 (2008).
- ²⁰⁶P. Dixon *et al.*, *Phys. Rev. Lett.* **102**, 173601 (2009).
- ²⁰⁷H. Hogan *et al.*, *Opt. Lett.* **36**, 1698 (2011).
- ²⁰⁸O. Magana-Loaiza *et al.*, *Phys. Rev. Lett.* **112**, 200401 (2014).
- ²⁰⁹F. Piacentini *et al.*, *Phys. Rev. Lett.* **116**, 180401 (2016).
- ²¹⁰F. Piacentini *et al.*, *Phys. Rev. Lett.* **117**, 170402 (2016).
- ²¹¹Y. Cho *et al.*, *Nat. Phys.* **15**, 665 (2019).
- ²¹²V. Gebhart *et al.*, e-print [arXiv:1905.01147](https://arxiv.org/abs/1905.01147) (2020).
- ²¹³J. Dressel *et al.*, *Rev. Mod. Phys.* **86**, 307 (2014).
- ²¹⁴D. J. Starling *et al.*, *Phys. Rev. A* **82**, 018002 (2010).
- ²¹⁵S. Xie *et al.*, *Appl. Phys. Express* **13**, 012001 (2020).
- ²¹⁶L. Li *et al.*, *Phys. Rev. A* **97**, 033851 (2018).
- ²¹⁷C. Fang *et al.*, *Appl. Phys. Lett.* **115**, 031101 (2019).
- ²¹⁸C. Marletto and V. Vedral, e-print [arXiv:2002.02777](https://arxiv.org/abs/2002.02777) (2021).
- ²¹⁹R. J. Adler *et al.*, *Phys. Lett. B* **477**, 424 (2000).
- ²²⁰Y. Jack Ng and H. van Dam, *Found. Phys.* **30**, 795 (2000).
- ²²¹C. Sabin, *Sci. Rep.* **7**, 716 (2017).